IOPscience iopscience.iop.org

This content has been downloaded from IOPscience. Please scroll down to see the full text.

Download details:

IP Address: 18.119.119.204
This content was downloaded on 03/05/2024 at 11:35

Please note that terms and conditions apply.

You may also like:

Simulation of Esterification-Transesterification of Waste Cooking Oil to Produce Biodiesel using Ultrasound Assisted Integrated Double Column Reactive Distillation
R D Kusumaningtyas, Y W P Budiono, A D H Kusuma et al.

An interview with Molly S Shoichet. Developing biomaterials and mobilizing resources for assaults on some of the most devastating medical problems
Myron Spector

Synthesis and Comparison of Chitosan and Methocel Based Flexible Gels for Potential Use As Organic Electrolytes in Batteries
Aswani Poosapati and Deepa Madan

IOP Publishing

Introduction to Nonlinear Optics of Photonic Crystals and Metamaterials (Second Edition)

Arthur R McGurn

Chapter 4

Basic properties of metamaterials

Metamaterials are engineered materials that include specific artificial mesoscopic features in their designs [1–5]. The mesoscopic features are introduced so as to tailor the material to exhibit specific permittivity and permeability properties when interacting with radiation of wavelengths greater than the mesoscopic inclusions. To such externally applied electromagnetic waves metamaterials appear homogeneous just as crystalline materials appear homogeneous for electromagnetic waves at optical wavelengths. The interest in the artificial mesoscopic inclusions is that they can be made to exhibit magnetic resonances at much higher frequencies of electromagnetic waves than those of the magnetic resonances of atoms and molecules of natural crystals [1]. This allows systems containing these features to exhibit high frequency regions of negative permeability, whereas atomic and molecular systems only display negative permeability at much lower frequencies than those of the metamaterials. The high frequency magnetic resonances when combined with a background dielectric medium of negative permittivity gives rise to metamaterials exhibiting a new property of negative refractive indices. Regions of frequencies with simultaneous negative permittivity and permeability have not been observed in naturally occurring materials and are only now available in designs of metamaterials and for certain configurations of photonic crystals. As a result the possibility of negative refractive index materials extends what was once considered a fundamental limitation on optical design. We shall see that the greater refractive properties found in materials with negative refractive indices extends refractive angles over a greater range of values.

In the following the properties of the basic split ring resonator (SRR) units forming metamaterials are explained along with how they can be arrayed in three dimensions to form bulk materials with engineered diamagnetic response properties. This is followed by a discussion of the properties of negative refractive index materials.

doi:10.1088/978-0-7503-3579-9ch4 © IOP Publishing Ltd 2021

4.1 Properties of SRRs and SRR arrays

The basic design of the inclusions engineered into metamaterials is an SRR [1–4]. There are many variations on the design that are made for engineering considerations, and the reader is referred to the literature and some remarks in the chapter 9 of this book for more details. In its basic design the SRR is a ring with a gap cut into it (see figure 4.1). The ring acts as an inductance and the gap acts as a capacitor so that the structure is an LC resonant circuit. The natural frequency of the SRR is then given by

$$\omega_0 = \frac{1}{\sqrt{LC}} \tag{4.1}$$

where L and C are the self-inductance and capacitance of the split ring, and this is the resonant frequency of the interaction of the SRR with an external driving electromagnetic wave. In addition to the self-inductance the neighboring rings in the metamaterial have a mutual inductance.

When an SRR is driven by an external electromagnetic wave of frequency, ω, as the wave frequency is passed through the natural frequency ω_0 of the SRR the SRR undergoes a resonant interaction with the wave [6–8]. To understand the operation of an SRR interacting with an external frequency-dependent wave consider the planar loop in figure 4.2(a) containing an inductor and a capacitor. From Faraday's law a time-dependent magnetic field perpendicular to the plane of the loop induces an electromotive force (emf) in the loop. In the figure the magnetic field is perpendicular to the page with the positive sense of the field out of the page, and the positive current in the loop is in the anti-clockwise direction. In the presence of the induced emf from the time-dependent field the circuit is essentially a forced LRC electromagnetic oscillator of the type shown in figure 4.2(b). The loop acts both as

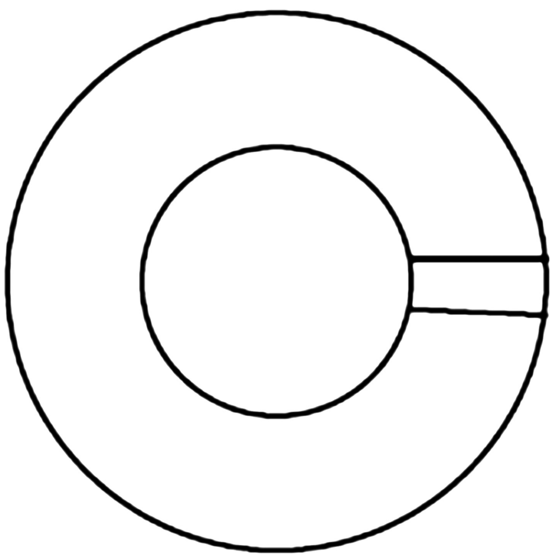

Figure 4.1. Basic design of an idealized SRR unit, a metallic ring with a gap filled with dielectric material.

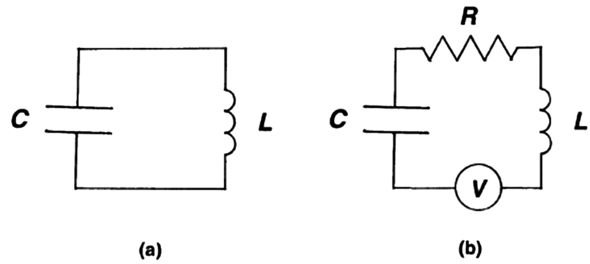

Figure 4.2. Schematics of: (a) an LC ring with a time varying magnetic field perpendicular to the plane of the ring, and (b) an LRC forced harmonic oscillator circuit.

the self-inductance of the circuit and the origin of the driving emf from its Faraday's law interaction with the external field. The equation of the driven oscillator is

$$L\frac{\mathrm{d}^2Q}{\mathrm{d}t^2} + R\frac{\mathrm{d}Q}{\mathrm{d}t} + \frac{Q}{C} = V \tag{4.2}$$

where Q is the charge on the capacitor and V is the forcing emf from Faraday's law.

For a magnetic field of the form $B(t) = B_0\cos\omega t$ the forcing emf in the LRC circuit is

$$V = V_0 \sin\omega t \tag{4.3}$$

where $V_0 = \omega A B_0$ for a loop of area A. From the theory of the LRC forced oscillator the response of the oscillator to the driving emf is given by the impendence of the circuit

$$Z(\omega) = \sqrt{R^2 + \left(\omega L - \frac{1}{\omega C}\right)^2} \tag{4.4}$$

relating the induced current in the circuit to the induced emf and the phase difference, φ, between the current and the driving emf

$$\varphi = \tan^{-1}\left(\frac{\omega L - \frac{1}{\omega C}}{R}\right). \tag{4.5}$$

Consequently, the current in the loop is given by

$$I(t) = I_0 \sin(\omega t - \varphi) \tag{4.6}$$

where

$$I_0 = \frac{V_0}{Z(\omega)}. \tag{4.7}$$

It is interesting to note that at the resonant condition $\omega = \omega_0 = \frac{1}{\sqrt{LC}}$ so that from (4.5) $\varphi = 0$, and the induced current and emf are in phase. Consequently, the time average resistive power losses in the circuit at resonance, $P_{\text{avg}} = \left(\frac{I_0}{\sqrt{2}}\right)^2 R = \left(\frac{V_0}{\sqrt{2}}\right)^2 \frac{R}{Z^2}$, are a maximum. In addition, the magnetic moment of the loop, μ, is given by

$$\mu(t) = I(t)A \tag{4.8}$$

and the potential energy of the interaction of the field with the dipole moment is

$$U(t) = -\mu(t)B(t). \tag{4.9}$$

Substituting in (4.9) gives

$$U(t) = -AI_0B_0 \cos(\omega t) \sin(\omega t - \varphi) \tag{4.10}$$

which on time average gives

$$\bar{U} = \frac{AI_0B_0}{2}\sin(\varphi). \tag{4.11}$$

From (4.11) it is seen that another consequence of the absence of a phase difference between the induced current and emf is that at resonance $U = 0$ and the effective magnetic moment of the loop is zero.

The regions of interest for metamaterial applications are at frequencies slightly above or below the resonant frequency. Expanding the frequency of the electromagnetic wave about the resonant frequency of the SRR

$$\omega = \omega_0 + \Delta\omega \tag{4.12}$$

gives from (4.5) the phase in terms of $\Delta\omega$

$$\varphi \approx 2\frac{L}{R}\Delta\omega \tag{4.13}$$

and from (4.4) the impedance

$$Z \approx R\sqrt{1+4\left(\frac{L}{R}\right)^2(\Delta\omega)^2} \tag{4.14}$$

in terms of $\Delta\omega$. From (4.13) and (4.14) the average power is given by

$$P_{\text{avg}} = \left(\frac{V_0}{\sqrt{2}}\right)^2 \frac{R}{Z^2} \approx \left(\frac{V_0}{\sqrt{2}}\right)^2 \frac{1}{R\left(1+4\left(\frac{L}{R}\right)^2(\Delta\omega)^2\right)} \tag{4.15}$$

so that for $\Delta\omega \neq 0$ the average power in (4.15) is less than at the $Z = R$ resonance condition.

In addition, from (4.11), (4.13), and (4.14) the average potential energy for the interaction with the magnetic field is

$$\bar{U} \approx AI_0B_0\frac{L}{R}\Delta\omega. \tag{4.16}$$

The sign of the average potential energy then depends on the sign of $\Delta\omega$. For positive $\Delta\omega$ the loop is diamagnetic and for negative $\Delta\omega$ the loop is paramagnetic. Defining the effective magnetic moment of the loop as

$$\mu_{\text{eff}} = -\frac{\bar{U}}{B_0} \tag{4.17}$$

gives the effective moment

$$\mu_{\text{eff}} = -\frac{L}{R^2}\frac{\omega A^2 B_0}{\sqrt{1+4\left(\frac{L}{R}\right)^2(\Delta\omega)^2}}\Delta\omega. \tag{4.18}$$

Near resonance the basic properties of the energy loss and effective magnetic moment of the SRR are simply related to the difference between the frequency of the electromagnetic wave and the SRR resonant frequency [2]. Plots of these properties are presented in figure 4.3. From (4.15) and figure 4.3(*a*) it is seen that the power loss

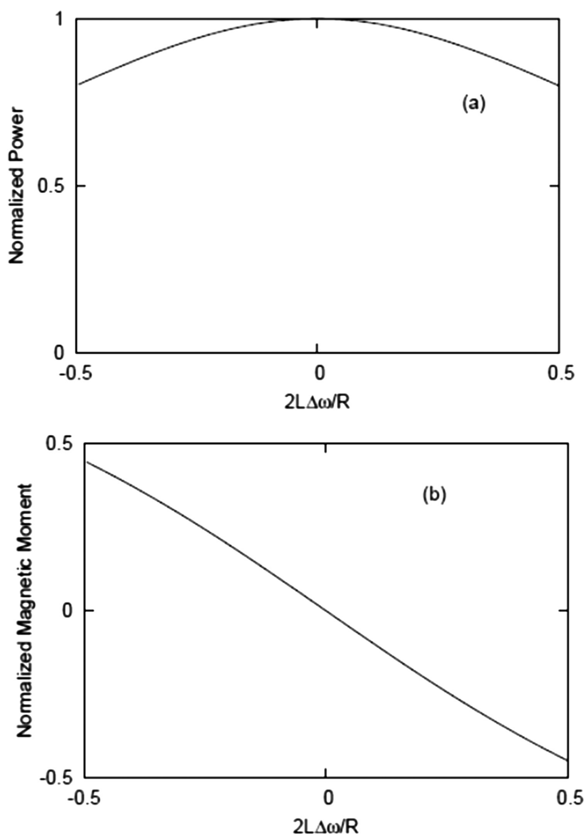

Figure 4.3. Power loss of the field to the SRR and the effective magnetic moment of the SRR: (a) the normalized power, $2RP_{\text{avg}}/V_0^2$, and (b) the normalized magnetic moment, $2R\mu_{\text{eff}}/\omega A^2 B_0$, both plotted versus $2L\,\Delta\,\omega/R$ where $\Delta\omega = 0$ at resonance.

in the *LRC* circuit exhibits a maximum at the $\Delta\omega = 0$ resonance condition while from (4.18) and its plot in figure 4.3(*b*) the effective magnetic moment passes through a sign change. By setting the values of $\frac{L\omega A^2 B_0}{R^2}$ for the amplitude and $\frac{L}{R}$ for the width of the resonance of the effective magnetic moment, the SRR passes through regions of enhanced paramagnetic and diamagnetic responses as the frequency of the electromagnetic wave passes through the SRR resonance. The region of enhanced diamagnetic response has been of great recent interest as in this region it is possible to use SRRs to facilitate the design of materials with negative permeability. In the additional presence of negative permittivity a negative refractive index is exhibited [3].

The results in figure 4.3 also illustrate a problem with the implementation of SRR metamaterials for their negative refractive index possibilities. The maximum of the losses in the materials occurs near the region of enhanced diamagnetism so that the region of losses can extend into the region of negative refractive index. It is one of the design problems of metamaterials to find ways of lessening the losses of the materials while obtaining a good negative index of refraction. The resonance nature of the negative index presents another design problem in that resonances are typically associated with instabilities of the system at a single frequency. This tends to limit the negative index effect to single frequencies, and the applications which are discussed later have predominantly been studied for narrow frequency bands.

For a material to display a negative index of refraction it must simultaneously have a negative permittivity and permeability [4, 5]. From the discussions above it is seen that a single SRR can be tuned to exhibit a negative permeability for an electromagnetic wave with a magnetic field polarized perpendicular to the plane of the SRR. To design a bulk material displaying a three-dimensional, homogeneous, isotropic diamagnetic response for electromagnetic waves propagating in a general direction within the bulk it is necessary to make an array of SRRs. An example of such a three-dimensional array is obtained by placing SRRs periodically in the x–y, y–z, and x–y planes of the bulk medium. This system of SRRs then forms a three-dimensional crystal with SRRs as the basis. The resonance conditions of the SRRs of the array are then tuned so that they give an enhanced diamagnetic response for waves with long wavelength compared to the size of the SRRs. This creates a bulk material with a negative permeability. To design a material with a negative refractive index it only remains to infuse into the SRR crystal a background material of negative permittivity. We now turn to a discussion of the properties of negative refractive index materials.

4.2 Negative refractive index metamaterials

To understand the nature of negative refractive materials begin by reviewing the solution for an electromagnetic plane wave propagating in a general electromagnetic medium [4, 5]. Consider a plane wave moving along the x-axis with $\vec{E}$ and $\vec{B}$ polarized, respectively, along the y- and z-axes. From Faraday's law

$$\frac{\partial E_y}{\partial x} = -\frac{\partial B_z}{\partial t} \tag{4.19}$$

and from Ampere's law

$$-\frac{\partial B_z}{\partial x} = \mu\varepsilon\frac{\partial E_y}{\partial t} + \mu\sigma E_y \tag{4.20}$$

where ε is the permittivity, μ is the permeability, and σ is a small conductivity. The plane wave solutions of (4.19) and (4.20) are of the form

$$E_y = E_0 \mathrm{e}^{\mathrm{i}(kx-\omega t)} \tag{4.21a}$$

and

$$B_z = B_0 \mathrm{e}^{\mathrm{i}(kx-\omega t)}. \tag{4.21b}$$

Substituting (4.21) into (4.19) and (4.20) gives the matrix equation for the field amplitudes

$$\begin{vmatrix} k & -\omega \\ -(\mu\varepsilon\omega + i\mu\sigma) & k \end{vmatrix} \begin{vmatrix} E_0 \\ B_0 \end{vmatrix} = 0 \tag{4.22a}$$

and the dispersion relation

$$k^2 - (\mu\varepsilon\omega^2 + i\mu\sigma\omega) = 0. \tag{4.22b}$$

For fixed $\omega > 0$ expanding to first order in σ gives

$$k = \pm\sqrt{\mu\varepsilon}\,\omega \pm \frac{i\mu\sigma}{2\sqrt{\mu\varepsilon}} \tag{4.23}$$

where the upper signs come from taking the square root to be a positive number and the lower signs come from taking the square root to be a negative number. The positive sign gives a phase velocity in the positive x-direction while the negative sign gives a phase velocity in the negative x-direction.

Substituting (4.23) into (4.21) gives

$$E_y = E_0 \mathrm{e}^{\mathrm{i}(\pm\sqrt{\mu\varepsilon}\,\omega x-\omega t)} \mathrm{e}^{\mp\frac{\mu\sigma}{2\sqrt{\mu\varepsilon}}x} \tag{4.24a}$$

and

$$B_z = B_0 \mathrm{e}^{\mathrm{i}(\pm\sqrt{\mu\varepsilon}\,\omega x-\omega t)} \mathrm{e}^{\mp\frac{\mu\sigma}{2\sqrt{\mu\varepsilon}}x} \tag{4.24b}$$

where for the upper sign

$$\begin{vmatrix} E_0 \\ B_0 \end{vmatrix} = \begin{vmatrix} \dfrac{1}{\sqrt{\mu\varepsilon}} \\ 1 \end{vmatrix} A \tag{4.25a}$$

and for the lower sign

$$\begin{vmatrix} E_0 \\ B_0 \end{vmatrix} = \begin{vmatrix} -\dfrac{1}{\sqrt{\mu\varepsilon}} \\ 1 \end{vmatrix} A. \tag{4.25b}$$

Here A is the amplitude of the magnetic induction.

From (4.24a) and (4.24b) it is seen that in the $\sigma \to 0$ limit the Poynting vector is given by

$$\vec{S} = \frac{1}{2}\frac{1}{\mu}\vec{E} \times \vec{B}^* = \pm\frac{1}{2}\frac{1}{\mu}\frac{1}{\sqrt{\mu\varepsilon}} \mid A \mid^2 \hat{i}. \tag{4.26}$$

From the form of the one-dimensional Poynting vector in (4.26) it is seen that the direction of the energy flow is determined by the sign of the permeability of the medium. In the case of a positive indexed material (i.e., for ε, $\mu > 0$) the flow of energy in the system is parallel to the wave vector of the plane wave where from (4.24) the wave vector is given by $\pm\ \mu\varepsilon\omega i$. In the case of a negative indexed material (i.e., for ε, $\mu < 0$) the flow of energy in the system is anti-parallel to the wave vector where the wave vector is again given by $\pm\ \mu\varepsilon\omega i$. Consequently, the signs of the one-dimensional wave vector and Poynting vector agree with one another in a positive indexed medium and are opposite one another in a negative index medium.

Including consideration of small non-zero conductivity in the electromagnetic solutions in (4.24) introduces a spatial decay term into the solutions. The spatial decay for both the electric field and the magnetic induction is given by $e^{\mp\frac{\mu\sigma}{2\sqrt{\mu\varepsilon}}x}$. In the case of a positive indexed material $\mu\sigma > 0$, and the amplitude of the waves decay in the direction of the energy flow. In addition, the energy flow is parallel to the direction of the wave vector. In the case of a negative indexed material $\mu\sigma < 0$, and the amplitude of the waves again decay in the direction of the energy flow. However, in this case the wave vector of the waves propagating in the negative indexed medium is now anti-parallel to the energy flow. The solutions for both the positive and negative indexed media make sense. In both cases they describe flows of energy which decay as the flow of energy advances through their respective media.

It may seem contradictory that for propagation in a negative refractive indexed medium the wave vector and Poynting vector are anti-parallel. This is not the case. To understand this, first consider a plane wave pulse of radiation propagating in a non-dissipative positive indexed medium. The pulse is localized in space and propagates as a spatially localized increase in energy that is moving in the direction of the wave vector. The wave vector and Poynting vector are parallel and the electric and magnetic energy density in the pulse are given, respectively, by

$$U_E = \frac{1}{2}\varepsilon \mid E(x,\, t)|^2 \tag{4.27a}$$

$$U_B = \frac{1}{2}\frac{1}{\mu} \mid B(x,\, t) \mid^2. \tag{4.27b}$$

In the absence of dispersion or for weak dispersion, the magnitude of the Poynting vector, giving the flow of energy in the direction of the wave vector, is related to the energies in (4.27) by

$$S = 2 \mid U_E \mid v = 2 \mid U_B \mid v \tag{4.28}$$

where v is the speed of light in the positive medium. Since ε, $\mu > 0$ the Poynting vector in (4.27) through (4.28) represents a net flow of positive energy carried by the pulse.

Now consider the flow of energy associated with a spatially localized field pulse moving in a negative indexed medium. Equations (4.27) and (4.28) also hold for such a pulse in the negative indexed medium. However, now $\varepsilon,\mu < 0$. The energy densities in (4.27) are negative and the pulse, written in the field amplitudes $|E(x, t)|$ and $|B(x, t)|$, shows up as a spatially localized decrease in energy. Though the pulse moves in a direction parallel to the wave vector, it is a pulse of energy decrease rather than a pulse of energy. In terms of the net energy in the system, a flow of negative energy past a point in space can be viewed as a flow of positive energy in the opposite direction. For the negative indexed medium, therefore, the amplitude of the Poynting vector in (4.28) represents a pulse of energy decrease traveling parallel to the wave vector or, equivalently, the flow of an energy pulse in the direction anti-parallel to the wave vector.

The flow of energy in positive and negative index media is similar to the flow of electrical current carried by the motion of holes and electrons in a semiconducting medium. In semiconductors, positive charged holes move parallel to the electric field to create the same electric current as negative charged electrons moving anti-parallel to the electric field. In the absence of an external magnetic field, the flow of the positive and negative charges cannot be distinguished. As shall be seen later, this analogy can be extended to considerations of the flow of light energy past an interface between a positive and negative index medium and the electrical current flow of electrons and holes through a p–n semiconductor junction. In these considerations a pulse of light energy is an energy particle in a positive indexed optical medium and a pulse of decrease of light energy is an energy hole in a negative indexed optical medium. The energy moves through the positive (negative) indexed medium by the motion of energy particles (energy holes), just as electrons carry the current in n-type semiconductors and holes carry the current in p-type semiconductors [9].

4.3 Refraction at the interface between positive and negative index media

As an example of the new properties introduced into optics by negative indexed materials, the refraction of light at the interface between positive and negative indexed media is considered [4, 5]. In a first case the refraction of light originating in the positive indexed medium is treated. This is followed by a treatment of the refraction of light originating in the negative indexed medium. Following these treatments a discussion is given of the design of a perfect lens.

4.3.1 Light originating in positive index media

Consider the planar interface between a positive and negative indexed medium. The positive indexed medium 1 (described by parameters μ_1, $\varepsilon_1 > 0$) is in the region $y > 0$, and the negative indexed medium 2 (described by parameters μ_2, $\varepsilon_2 < 0$) is in the region $y < 0$.

In terms of the angles defined in figure 4.4 the wave incident on the interface from medium 1 is given by

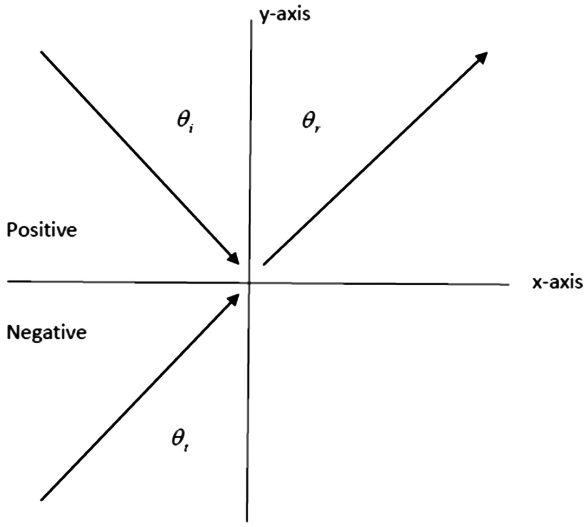

Figure 4.4. Refraction at a planar interface for incident light in a positive medium and refracted light in a negative medium. The arrows indicate the wave vectors and as represented in the figure θ_i, θ_r, $\theta_\mathrm{t} > 0$.

$$\vec{E}_\mathrm{I} = E_\mathrm{I}(\cos\theta_\mathrm{i}\hat{i} + \sin\theta_\mathrm{i}\hat{j})\mathrm{e}^{\mathrm{i}[k(\sin\theta_\mathrm{i}x - \cos\theta_\mathrm{i}y) - \omega t]} \tag{4.29a}$$

$$\vec{B}_\mathrm{I} = E_\mathrm{I}\frac{k}{\omega}\hat{k}\mathrm{e}^{\mathrm{i}[k(\sin\theta_\mathrm{i}x - \cos\theta_\mathrm{i}y) - \omega t]} \tag{4.29b}$$

and the reflected wave in medium 1 is given by

$$\vec{E}_\mathrm{R} = E_\mathrm{R}(-\cos\theta_\mathrm{r}\hat{i} + \sin\theta_\mathrm{r}\hat{j})\mathrm{e}^{\mathrm{i}[k(\sin\theta_\mathrm{r}x + \cos\theta_\mathrm{r}y) - \omega t]} \tag{4.30a}$$

$$\vec{B}_\mathrm{R} = E_\mathrm{R}\frac{k}{\omega}\hat{k}\mathrm{e}^{\mathrm{i}[k(\sin\theta_\mathrm{r}x + \cos\theta_\mathrm{r}y) - \omega t]} \tag{4.30b}$$

where

$$k = \sqrt{\mu_1\varepsilon_1}\omega. \tag{4.31}$$

The wave vectors of the incident and reflected waves are

$$\vec{k}_\mathrm{i} = k(\sin\theta_\mathrm{i}, -\cos\theta_\mathrm{i}, 0) \tag{4.32a}$$

$$\vec{k}_\mathrm{r} = k(\sin\theta_\mathrm{r}, \cos\theta_\mathrm{r}, 0) \tag{4.32b}$$

and their respective Poynting vectors are

$$\vec{S}_\mathrm{I} = \frac{1}{2}\frac{1}{\mu_1}\frac{1}{\omega} \mid E_\mathrm{I} \mid^2 \vec{k}_\mathrm{i} \tag{4.33a}$$

$$\vec{S}_\mathrm{R} = \frac{1}{2}\frac{1}{\mu_1}\frac{1}{\omega} \mid E_\mathrm{R} \mid^2 \vec{k}_\mathrm{r}. \tag{4.33b}$$

Equations (4.32) and (4.33) show the standard result of energy flow into and out of the interface between the two media. Since $\mu_1 > 0$ the Poynting vectors of both the incident and reflected waves are parallel to their respective wave vectors.

For the case in which medium 2 is a negative indexed medium (i.e., $\varepsilon_2, \mu_2 < 0$) care must be taken to choose a solution in medium 2 representing an energy flow away from the interface. The correct form of the solution for the transmitted wave under these conditions is given by

$$\vec{E}_{\mathrm{T}} = E_{\mathrm{T}}(-\cos\theta_{\mathrm{t}}\hat{i} + \sin\theta_{\mathrm{t}}\hat{j})\mathrm{e}^{\mathrm{i}[q(\sin\theta_{\mathrm{t}}x + \cos\theta_{\mathrm{t}}y) - \omega t]} \tag{4.34a}$$

$$\vec{B}_{\mathrm{T}} = E_{\mathrm{T}}\frac{q}{\omega}\hat{k}\mathrm{e}^{\mathrm{i}[q(\sin\theta_{\mathrm{t}}x + \cos\theta_{\mathrm{t}}y) - \omega t]} \tag{4.34b}$$

where we use the angles as defined by figure 4.4 for the case of a negative medium 2. Specifically, the positive angle θ_{t} must be in the third quadrant and measured from the y-axis. The transmitted wave in equation (4.34) now has a wave vector and a Poynting vector of the respective forms

$$\vec{q}_{\mathrm{t}} = q(\sin\theta_{\mathrm{t}}, \cos\theta_{\mathrm{t}}, 0) \tag{4.35}$$

where $q = \sqrt{\mu_2\varepsilon_2}\,\omega$, and

$$\vec{S}_{\mathrm{T}} = \frac{1}{2}\frac{1}{\mu_2}\frac{1}{\omega} \mid E_{\mathrm{T}} \mid^2 \vec{q}_{\mathrm{t}} \tag{4.36}$$

which for $\mu_2 < 0$ represent an energy flow away from the interface and into the third quadrant.

For a comparison, consider the case in which medium 2 is positive indexed (i.e., $\varepsilon_2, \mu_2 > 0$) rather than negative indexed. Now the transmitted wave in medium 2 is given by

$$\vec{E}_{\mathrm{T}} = E_{\mathrm{T}}(\cos\theta_{\mathrm{t}}\hat{i} + \sin\theta_{\mathrm{t}}\hat{j})\mathrm{e}^{\mathrm{i}[q(\sin\theta_{\mathrm{t}}x - \cos\theta_{\mathrm{t}}y) - \omega t]} \tag{4.37a}$$

$$\vec{B}_{\mathrm{T}} = E_{\mathrm{T}}\frac{q}{\omega}\hat{k}\mathrm{e}^{\mathrm{i}[q(\sin\theta_{\mathrm{t}}x - \cos\theta_{\mathrm{t}}y) - \omega t]} \tag{4.37b}$$

where, in the case of a positive medium 2, the positive angle θ_{t} must be in the fourth quadrant and measured from the y-axis. The wave vector and Poynting vector of the transmitted wave, respectively, are given by

$$\vec{q}_{\mathrm{t}} = q(\sin\theta_{\mathrm{t}}, -\cos\theta_{\mathrm{t}}, 0) \tag{4.38}$$

$$\vec{S}_{\mathrm{T}} = \frac{1}{2}\frac{1}{\mu_2}\frac{1}{\omega} \mid E_{\mathrm{T}} \mid^2 \vec{q}_{\mathrm{t}} \tag{4.39}$$

where

$$q = \sqrt{\mu_2\varepsilon_2}\,\omega. \tag{4.40}$$

Since $\mu_2 > 0$ it is seen that the wave vector and Poynting vector are parallel, and the energy of the transmitted wave correctly flows away from the interface and into the fourth quadrant.

It is interesting to note the similarity of the solutions in (4.34) through (4.36) for the negative indexed medium 2 with those of the reflected wave for the positive indexed medium 1 given in (4.30), (4.32b), and (4.33b). In particular, both solutions have wave vectors with positive y-components. Due to the sign difference between $\mu_1 > 0$ and $\mu_2 < 0$, however, the two solutions represent energy flows away from the $y = 0$ plane in opposite directions along the y-axis. Specifically, it is seen from (3.35) and (4.36) that for $\mu_2 < 0$ the wave vector and Poynting vectors of the transmitted wave are anti-parallel. Though the wave vector has a positive component along the y-axis, from (4.36) the energy flow of the transmitted wave is in the negative y-direction, away from the interface. In the case of the reflected wave, however, the wave vector and Poynting vectors are parallel and the reflected wave has an energy flow along the positive y-axis.

In addition, it should be noted that, due to the translational symmetry of the planar interface at $y = 0$ between media 1 and 2, the solutions in (4.29), (4.30), (4.34), and (4.37) all have wave vectors with equal x-components. This requires that $\theta_i = \theta_r$ and $k\sin\theta_i = q\sin\theta_t$. These results arise solely from the translational symmetry and are independent of whether or not media 1 and 2 are positive or negative indexed materials.

To obtain the electric field amplitudes in these solution forms it is necessary to match the boundary conditions at the interface between the two media. From the continuity of the component of the electric field tangent to the interface it follows that

$$E_I - E_R = \alpha E_T \tag{4.41a}$$

where $\alpha = \frac{\cos\theta_t}{\cos\theta_i}$ when medium 2 has a positive index and $\alpha = -\frac{\cos\theta_t}{\cos\theta_i}$ when medium 2 has a negative index. From the continuity of the component of the magnetic field tangent to the interface it follows that

$$E_I + E_R = \beta E_T \tag{4.41b}$$

where $\beta = \frac{\mu_1\sqrt{\mu_2\varepsilon_2}}{\mu_2\sqrt{\mu_1\varepsilon_1}}$ when medium 2 is either negative or positive indexed. Solving these gives

$$E_T = \frac{2}{\alpha + \beta}E_I \tag{4.42a}$$

$$E_R = \frac{\beta - \alpha}{\alpha + \beta}E_I. \tag{4.42b}$$

4.3.2 Light originating in negative indexed media

Next, consider the planar interface between a negative indexed medium 1 (i.e., μ_1, $\varepsilon_1 < 0$) in the region $y > 0$, and the positive indexed medium 2 (i.e., μ_2, $\varepsilon_2 > 0$) is in the region $y < 0$. The incident wave is now in the negative indexed medium and the transmitted wave is in the positive indexed medium [4, 5].

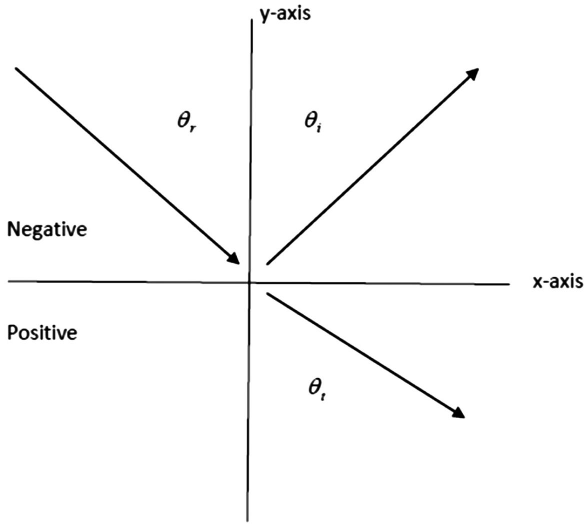

Figure 4.5. Refraction at a planar interface for incident light in a negative medium and refracted light in a positive medium. The arrows indicate the wave vectors and as represented in the figure θ_{i}, θ_{r}, $\theta_{\mathrm{t}} > 0$.

In terms of the angles defined in figure 4.5 the wave incident on the interface from medium 1 is given by

$$\vec{E}_{\mathrm{I}} = E_{\mathrm{I}}(\cos\theta_{\mathrm{i}}\hat{i} - \sin\theta_{\mathrm{i}}\hat{j})e^{i[k(\sin\theta_{\mathrm{i}}x+\cos\theta_{\mathrm{i}}y)-\omega t]} \tag{4.43a}$$

$$\vec{B}_{\mathrm{I}} = -E_{\mathrm{I}}\frac{k}{\omega}\hat{k}e^{i[k(\sin\theta_{\mathrm{i}}x+\cos\theta_{\mathrm{i}}y)-\omega t]} \tag{4.43b}$$

and the reflected wave in medium 1 is given by

$$\vec{E}_{\mathrm{R}} = E_{\mathrm{R}}(\cos\theta_{\mathrm{r}}\hat{i} + \sin\theta_{\mathrm{r}}\hat{j})e^{i[k(\sin\theta_{\mathrm{r}}x-\cos\theta_{\mathrm{r}}y)-\omega t]} \tag{4.44a}$$

$$\vec{B}_{\mathrm{R}} = E_{\mathrm{R}}\frac{k}{\omega}\hat{k}e^{i[k(\sin\theta_{\mathrm{r}}x-\cos\theta_{\mathrm{r}}y)-\omega t]} \tag{4.44b}$$

where

$$k = \sqrt{\mu_1\varepsilon_1}\,\omega. \tag{4.45}$$

The wave vectors of the incident and reflected waves are now, respectively,

$$\vec{k}_{\mathrm{i}} = k(\sin\theta_{\mathrm{i}}, \cos\theta_{\mathrm{i}}, 0) \tag{4.46a}$$

$$\vec{k}_{\mathrm{r}} = k(\sin\theta_{\mathrm{r}}, -\cos\theta_{\mathrm{r}}, 0) \tag{4.46b}$$

with Poynting vectors

$$\vec{S}_{\mathrm{I}} = \frac{1}{2}\frac{1}{\mu_1}\frac{1}{\omega} \mid E_{\mathrm{I}} \mid^2 \vec{k}_{\mathrm{i}} \tag{4.47a}$$

$$\vec{S}_R = \frac{1}{2}\frac{1}{\mu_1}\frac{1}{\omega} \mid E_R \mid^2 \vec{k}_r \tag{4.47b}$$

respectively. Equations (4.46) and (4.47) show the standard result of energy flow into and out of the interface of the two media. Since $\mu_1 < 0$ both incident and reflected wave Poynting vectors are anti-parallel to the wave vectors of their respective waves. This is a general property of propagation in a negative indexed medium.

For the present case of a positive indexed medium (i.e., ε_2, $\mu_2 > 0$) the transmitted wave in medium 2 is given by

$$\vec{E}_T = E_T(\cos\theta_t\hat{i} + \sin\theta_t\hat{j})e^{i[q(\sin\theta_t x - \cos\theta_t y) - \omega t]} \tag{4.48a}$$

$$\vec{B}_T = E_T\frac{q}{\omega}\hat{k}e^{i[q(\sin\theta_t x - \cos\theta_t y) - \omega t]} \tag{4.48b}$$

with the wave vector and Poynting vector of the transmitted wave, respectively, given by

$$\vec{q}_t = q(\sin\theta_t, -\cos\theta_t, 0) \tag{4.49}$$

$$\vec{S}_T = \frac{1}{2}\frac{1}{\mu_2}\frac{1}{\omega} \mid E_T \mid^2 \vec{q}_t \tag{4.50}$$

and where

$$q = \sqrt{\mu_2\varepsilon_2}\,\omega. \tag{4.51}$$

Since $\mu_2 > 0$ the wave vector and Poynting vectors are parallel, and the energy of the transmitted wave correctly flows away from the interface.

Again, the translational symmetry along the interface of the two media requires the x-components of the wave vectors of the incident, reflected, and transmitted waves to be equal. From this it follows that $\theta_i = \theta_r$ and $k\sin\theta_i = q\sin\theta_t$. Upon an application of the boundary conditions between the two media: (i) the continuity of the component of the electric field tangent to the interface requires

$$E_I + E_R = \alpha E_T \tag{4.52a}$$

where $\alpha = \frac{\cos\theta_t}{\cos\theta_i}$ when medium 1 is negative indexed and medium 2 is positive indexed. (ii) At this same interface, the continuity of the components of the magnetic field tangent to the interface requires

$$-E_I + E_R = \beta E_T \tag{4.52b}$$

where $\beta = \frac{\mu_1\sqrt{\mu_2\varepsilon_2}}{\mu_2\sqrt{\mu_1\varepsilon_1}}$. Solving these gives

$$E_T = \frac{2}{\alpha - \beta}E_I \tag{4.53a}$$

$$E_R = \frac{\alpha + \beta}{\alpha - \beta}E_I. \tag{4.53b}$$

4.3.3 Semiconductor analogy

The refraction of light at the interfaces between the positive and negative indexed media can be described in analogy with electrical current moving through an n–p or p–n semiconductor junction [9].

For light incident on the interface from the positive indexed medium an energy pulse is sent towards the interface. As the pulse travels to the interface it interacts with an energy hole coming towards the surface from the negative indexed medium. The hole, propelled in the negative indexed medium towards the interface, exists in response to the field from the incident pulse at the interface. At the interface the incident energy pulse and the hole destroy one another in the process of creating an energy pulse that is reflected from the surface into the positive indexed medium. The net result in the final state of the system is energy moving away from the surface in both the positive and negative indexed media.

For light incident on the interface from the negative indexed medium an energy hole travels away from the interface, creating an energy flow towards the interface. The field at the interface arising from the hole causes an energy pulse to be created at the interface. This pulse moves away from the interface and into the positive indexed medium. In addition, the fields at the interface create a hole traveling towards the interface through the negative indexed medium. The hole traveling towards the interface describes the energy reflected from the interface. The net result in the final state of the system is energy moving away from the interface and into both the positive and negative indexed media.

It is seen for both types of interfaces the energy transport properties are governed separately by the nature of the energy pulses in the positive medium and the nature of the energy holes in the negative indexed medium. The energy currents are parallel to the wave vector in the positive indexed medium and anti-parallel to the wave vector in the negative indexed medium. The energy pulses and holes in part destroy one another at the interface to give rise to various reflected and transmitted flows of energy.

4.3.4 The perfect lens

In traditional optics the refraction of light at the interface between different media is commonly used to make a focusing lens [8, 10]. The focusing lens directs light incident on it from an object in such a manner so as to create an image of the object. The resulting flow of light then appears to come from the created image rather than the original object. There are many problems in designing a lens that gives a good image, i.e., a nicely focused representation of the object. Some of these problems include: the curve of the surface, the dispersive properties of the media, and the presence of imperfections in the design and the materials [11].

One fundamental problem in the optics of positive indexed materials is that the refraction of a ray of light incident on a planar interface from the first or second quadrant can only be refracted into the third or fourth quadrants, respectively [3, 11]. A consequence of this is that to form a focusing lens from a positive index material requires at least one concave or convex curved surface. The curvature allows for the additional bending of the light ray which cannot be accomplished by the dielectric mismatch at a series of planar surfaces. As a result of the curvature of the lens surfaces, the two surfaces intersect one another in a circle of radius R which is the aperture of the lens. The finite size of the aperture of the lens is a fundamental limitation on the resolution of the image formed by the lens. Specifically, only wavelengths less that the diameter of the lens can leave the object, pass through the lens, and arrive at the focus of the lens. A precise criterion for the focusing power of a lens is that in forming an image of an object, only wavelengths of light, λ, satisfying

$$\lambda < R \tag{4.54}$$

are resolved in the focused image of the object. Such a lens is basically imperfect because of the limitation of its focusing ability arising from its finite R. To give a perfect image of the object, the image formed by the lens should contain all Fourier components of light rather than a restricted subset.

The new optics of negative indexed materials does not suffer from the necessity of making lenses of finite apertures. This follows from our earlier discussions of the refraction of light from a positive indexed medium to a negative indexed medium. In the optics of negative indexed materials the refraction of a ray of light incident on a planar interface from the first or second quadrant of a positive indexed medium is refracted into the fourth or third quadrants of the second negative indexed medium, respectively. This means that the additional beam bending arising from a curved surface between the two media is not necessary. In addition, from our earlier discussions of the refraction of light from a negative indexed medium to a positive indexed medium: the refraction of a ray of light incident on a planar interface from the first or second quadrant of a negative indexed medium is refracted into the fourth or third quadrants of the second positive indexed medium, respectively. This again precludes the need for additional bending from a curved surface.

In principle a slab of negative indexed medium surrounded by a positive indexed medium can form a lens with perfect resolution. The system can be used to focus an image–object pair in the positive indexed medium on the opposite sides of the slab. Since the slab is of infinite extent with an infinite aperture (i.e., $R \to \infty$) the lens is able to focus all propagating wavelength components of the object in its image. In addition the permittivity and permeability can be adjusted so that even the evanescent components of light from the object are reassembled at the image, giving a complete characterization in the image of the object [10]. In principle an image with perfect resolution can be formed by imaging with an infinite slab of negative index medium. The lens in this sense is a perfect lens. It is important to note, however, that due to the magnetic resonance origins of engineered negative indexed materials, the perfect lens model has some additional complications in its experimental realization. Resonances with negative permeabilities only exist over a band of frequencies. Also, resonances are associated with dielectric losses which become greater near the frequency peak of the resonance. Consequently, the idea of a perfect lens has only been very narrowly realized experimentally.

In addition, negative indexed media can allow for the development of an electromagnetic cloaking. Using a gradual spatial variation of the refractive index in an engineered medium, light can be steered around an object hidden in the medium and sent off parallel to its original direction before it encountered the cloaking device [8]. To do this requires the use of both positive and negative indexed media in order to accomplish all of the bending of light required of the cloaking device. Due to the restrictions from magnetic resonance effects, this has only been done for the case of a single frequency of incident light. Using the idea of a medium with a spatial variation of positive and negative index, suggestions for the mimicking of certain optical effects in general relativity have also been proposed [12–14].

4.3.5 Radiation in negative indexed media

Another example of new effects associated with negative indexed media involves the properties of radiation fields generated within them. In this subsection, the radiation fields of an electric dipole antenna located in a negative indexed medium and of a point change moving within a negative index medium are treated [5, 15]. An important determiner of the properties of the radiation fields comes from the fact that the wave vector and Poynting vector of the radiation in a negative indexed medium are anti-parallel.

In the Lorentz gauge (i.e., $\nabla \bullet \vec{A} = -\frac{1}{c_{\mathrm{m}}^2}\frac{\partial V}{\partial t}$) the radiation equations for electromagnetic waves generated from a source are [15]

$$\nabla^2 V - \frac{1}{c_{\mathrm{m}}^2}\frac{\partial^2 V}{\partial t^2} = -\frac{1}{\varepsilon}\rho \tag{4.55a}$$

$$\nabla^2 \vec{A} - \frac{1}{c_{\mathrm{m}}^2}\frac{\partial^2 \vec{A}}{\partial t^2} = -\mu\vec{J} \tag{4.55b}$$

where $(\vec{A}(\vec{r}, t), V(\vec{r}, t))$ are the vector and scalar potentials and $(\vec{J}(\vec{r}, t), \rho(\vec{r}, t))$ are the current and charge densities of the source and c_{m} is the speed of light in the medium. The solutions of (4.55) are

$$V_{\mp}(\vec{r}, t) = \frac{1}{4\pi\varepsilon}\int\frac{\rho(\vec{r}\,', t_{\mp})}{|\vec{r} - \vec{r}\,'|}\mathrm{d}^3r' \tag{4.56a}$$

$$\vec{A}_{\mp}(\vec{r}, t) = \frac{\mu}{4\pi}\int\frac{\vec{J}(\vec{r}\,', t_{\mp})}{|\vec{r} - \vec{r}\,'|}\mathrm{d}^3r' \tag{4.56b}$$

where $t_{\mp} = t \mp \frac{|\vec{r} - \vec{r}\,'|}{c_{\mathrm{m}}}$. In (4.56) the upper (lower) signs are known as the retarded (advanced) potentials of the fields generated by the source terms. For positive indexed media the radiation fields describing the motion of radiation away from the sources are obtained from the retarded potentials. Later, we shall see that the advanced potentials are those of interest for radiation generated in a negative indexed medium.

The electric field and the magnetic induction are then obtained from the vector and scalar potentials as

$$\vec{E} = -\nabla V - \frac{\partial \vec{A}}{\partial t} \tag{4.57a}$$

and

$$\vec{B} = \nabla \times \vec{A} \tag{4.57b}$$

respectively. Note that in (4.56) as $c_m \to \infty$ the potentials, appropriately, reduce to the scalar and vector potentials of static electric and magnetic fields.

As an example of the formulation consider an electric point dipole source located at the origin of coordinates and having the form of a harmonic time-dependent electric dipole given by $\vec{p}(t) = p_0 \cos(\omega t)\hat{k}$. In the far field limit in which the point of observation is a great distance (i.e., $kr \gg 1$) from the source, the electric field and magnetic induction generated by the time-dependent dipole are

$$\vec{E} = -\frac{\mu p_0 \omega^2}{4\pi} \frac{\sin\theta}{r} \cos\omega\left(t \mp \frac{r}{c_m}\right)\hat{\theta} \tag{4.58a}$$

$$\vec{B} = \mp\frac{\mu p_0 \omega^2}{4\pi c_m} \frac{\sin\theta}{r} \cos\omega\left(t \mp \frac{r}{c_m}\right)\hat{\varphi} \tag{4.58b}$$

where (r,θ,φ) are the standard polar coordinates centered at the origin of coordinates. From (4.58) the Poynting vector of the radiation fields is

$$\langle \vec{S} \rangle = \pm \frac{\mu p_0^2 \omega^4}{32\pi^2 c_m} \frac{\sin^2\theta}{r^2}\hat{r} \tag{4.59}$$

giving an average power

$$\langle P \rangle = \pm \frac{\mu}{12\pi} \frac{p_0^2 \omega^4}{c_m}. \tag{4.60}$$

For a positive indexed medium the permeability is positive and the upper sign from the retarded solution gives an energy flow away from the dipole source. For a negative indexed medium the permeability is negative and the lower sign from the advanced solution gives an energy flow away from the dipole source.

An additional important case is that of the determination of the radiation from a point charge accelerating in a dielectric medium. To handle this system, first consider the radiation characteristics of a general time-dependent localized charge distribution, given by (4.56). The results for a general charge and current density are then immediately specialized to the problem of a single accelerating point charge. In the case that $r' \ll r$, for a charge distribution located about the origin of coordinates, the non-relativistic limit of (4.56) becomes

$$V_{\mp}(\vec{r}, t) = \frac{1}{4\pi\varepsilon}\left[\frac{Q}{r} + \frac{\hat{r} \bullet \vec{p}(t_{\mp})}{r^2} + \frac{\hat{r} \bullet \dot{\vec{p}}(t_{\mp})}{c_m r}\right] \tag{4.61a}$$

$$\vec{A}_{\mp}(\vec{r}, t) = \frac{\mu}{4\pi}\frac{\vec{\dot{p}}(t_{\mp})}{r} \quad . \tag{4.61b}$$

Here Q is the net charge of the distribution and $\vec{p}(t)$ is the electric dipole moment of the charge distribution about the origin of coordinates.

For the accelerating point charge it is only needed to determine the electric dipole moment of the charge relative to the origin of coordinates. It then follows that the radiation fields of the charge distribution are

$$\vec{E}(r, \theta, \varphi, t_{\mp}) = \frac{\mu}{4\pi}\vec{\ddot{p}}(t_{\mp})\frac{\sin\theta}{r}\hat{\theta} \tag{4.62a}$$

$$\vec{B}(r, \theta, \varphi, t_{\mp}) = \pm\frac{\mu}{4\pi}\frac{\vec{\ddot{p}}(t_{\mp})}{c_{\mathrm{m}}}\frac{\sin\theta}{r}\hat{\varphi} \tag{4.62b}$$

where (r, θ, φ) are standard polar coordinates chosen so that the charge is accelerating along the z-axis. The Poynting vector of these radiation fields is

$$\vec{S} = \pm\frac{\mu[\ddot{p}(t)]^2}{16\pi^2 c_{\mathrm{m}}}\frac{\sin^2\theta}{r^2}\hat{r} \tag{4.63}$$

giving a net radiated power

$$P = \pm\frac{\mu}{6\pi}\frac{q^2 a^2(t)}{c_{\mathrm{m}}} \tag{4.64}$$

where $a(t)$ is the acceleration of the charge. For a positive indexed medium the permeability and permittivity are positive. In this case, the upper sign from the retarded solution gives an energy flow away from the dipole source. For a negative indexed medium the permeability and permittivity are negative and the lower sign from the advanced solution gives an energy flow away from the dipole source. Again, in the positive indexed medium the Poynting vector and wave vector are parallel while they are anti-parallel in the negative indexed medium.

References

[1] Cai W and Shalaev V 2001 *Optical Metamaterials: Fundamental and Applications* (New York: Springer)

[2] Engheta N and Ziolkowski R W (ed) 2006 *Metamaterials: Physics and Engineering Explorations* (New York: Wiley-IEEE)

[3] Ramakrishna S A 2005 Physics of negative index materials *Rep. Prog. Phys.* **68** 449

[4] Veselago V G 1968 The electrodynamics of substances with simultaneously negative values of ε and μ *Sov. Phys.– Usp.* **10** 509

[5] Agranovich V M 2006 Hybrid organic–inorganic nanostructures and light–matter interaction *Problems of Condensed Matter Physics* ed A L Ivanov and S G Tikhodeev (Oxford: Clarendon) ch 2

[6] Eleftheriou M, Lazarides N and Tsironis G P 2008 Magnetoinductive breathers in metamaterials *Phys. Rev.* E **77** 036608

[7] Eleftheriades G V 2009 EM transmission-line metamaterials *Mater. Today* **12** 30
[8] Kourakis I, Lazarides N and Tsironis G P 2007 Self-focusing and envelope pulse generation in nonlinear magnetic metamaterials *Phys. Rev.* E **75** 067601
[9] Marder M P 2010 *Condensed Matter Physics* 2nd edn (Hoboken, NJ: Wiley)
[10] Pendry J B 2000 Negative refraction makes a perfect lens *Phys. Rev. Lett.* **85** 3966
[11] Smith W J 2007 *Modern Optical Engineering* 4th edn (New York: McGraw-Hill)
[12] Leonhardt U and Philibin T G 2006 General relativity in electrical engineering *New J. Phys.* **8** 247
[13] Leonhardt U and Philibin T G 2009 Transformation optics and the geometry of light *Prog. Opt.* **52** 69
[14] Van B J 1984 *Relativity and Engineering* (Berlin: Springer)
[15] Jackson J D 1999 *Classical Electrodynamics* 3rd edn (New York: Wiley)